Experimental and modeling approach to study separation of water in crude oil emulsion under non-uniform electrical field

Kazem Alinezhad*,**,†, Morteza Hosseini*, Kamyar Movagarnejad*, and Mehdi Salehi***

*Chemical Engineering Department, Mazandaran University, Mazandaran, Iran
**Iranian Offshore Oil Company (IOOC), Lavan Island, Iran
***Iranian Offshore Oil Company (IOOC), Khark Island, Iran

Abstract−In many ways, the use of high electrostatic fields in the separation of water-in-oil emulsions is a mature technology, with most developments arising from attempts to improve the process of crude oils, in terms of the separation of water, salt or other hydrophilic impurities. In this way, different mechanisms have been proposed until now and several parameters have been studied to estimate the level of separation. In this work, after a review of the process and its application, new results are presented for AC currents under non-uniform electrical fields (dielectrophoresis) on the water-in-crude oil emulsion. Then the effects of voltage, temperature, volume fraction and API are studied on degree of separation. Finally, a correlation is presented among these parameters by an experimental model.

Key words: Dielectrophoresis, Non-uniform Electrical Field, Water-in-crude Oil Emulsion

INTRODUCTION

Emulsions of crude oil and water can be encountered at many stages during drilling, producing, transporting and processing of crude oils and in many locations such as in hydrocarbon reservoirs, well bores, surface facilities, transportation systems and refineries. Water or brine typically accompanies crude oil during its recovery from a reservoir. Emulsions form as a result of the presence of water coupled with the application of high shear stresses at the wellhead and choke valves [1,2]. The presence of the emulsion is beneficial for the extraction process, but it poses major problems for the additional refining steps [3,4]. Water dispersed as small droplets in crude oil and most of the salts are dissolved in water droplets in crude oil. Since this water is a salt carrier, the terms dehydration and desalting are used synonymously. The accumulation of surface-active molecules and inorganic solids from the crude at the oil-water interface produce a mechanically strong, rigid, viscoelastic stagnant film that resists droplet coalescence [1,5-8]. If these impurities, such as water and salt included in the crude oil, were not removed, they would cause serious corrosion and fouling in the heat exchanger and distillation equipment. Also, if allowed to pass through refinery operations, emulsified water would corrode refinery equipment, such as overhead distillation columns, and poison catalysts as a result of dissolved salts [7,9,10]. Therefore demulsification is an essential industrial process, mainly used for removing water and salts from crude oil. To date, there exist several techniques for enhancing the separation of water-in-oil emulsions, such as the addition of chemical demulsifier [54], pH adjustment [11], gravity or centrifugal settling [12], filtration [11], heat treatment and electrostatic demulsification [2,13]. The electrostatic demulsification method in a high-voltage field is one of the most effective and the simplest demulsi-

fication methods. By observations under a microscope, it became clear that electrostatic forces caused the coalescence of fine water drops and their growth to larger drops, which then readily fell by electrostatic forces or gravity [14-17]. The first application of electrostatic force involved the treatment of aerosols, as in the removal of dust from air, in which the so-called Cottrell Precipitator was used to good effect. The application of electrostatic fields has usually followed a particular need, and Cottrell used the precedence of his dust-collector for dehydration of crude oil emulsions in US oil-fields in 1911 [18]. This efficient demulsification process can be achieved with DC, AC and pulsed DC fields. Therefore, it is necessary to further the knowledge of coalescence mechanism and electrical field. In this way, different mechanisms have been proposed until now and several parameters have been studied for estimating the level of separation. Because of the many parameters to be examined, e.g. operating conditions (voltage, frequency, temperature) and emulsion properties (density, viscosity, water drop size, hold up), a complete rate equation which takes into account all these factors has not yet been presented. In this article, we will investigate some of the main characteristics of crude oil emulsions, in particular the adsorbed layer properties of amphiphilic molecules and properties of films between drops in *W/O* emulsion and continuously the effect of some factors such as type of the electrode, degree of *API*, volume fraction, temperature and voltage on the separation rate of water from crude oil (as the separation efficiency) by a glass batch electrostatic dehydrator in a non-uniform electric field. Finally, an experimental model is presented by these parameters.

BACKGROUND

1. Surface-active Species in Crude Oil

Many advancements have been made in the field of emulsions in recent years. Emulsion behavior is largely controlled by the properties of the adsorbed layers that stabilize the oil-water surfaces.

---

†To whom correspondence should be addressed.
E-mail: kazem_alinezhad@yahoo.com

The complexity of petroleum emulsions comes from the oil composition in terms of surface-active molecules contained in the crude, such as low molecular weight fatty acids, naphthenic acids and asphaltenes. These molecules can interact with each other and reorganize at oil/water interfaces and produce a mechanically strong, rigid, viscoelastic stagnant film that resists droplet coalescence. This skin is formed through the interactions of surface-active molecules in the crude, which fall into two main categories, asphaltenes and resins [19-22].

Boussingault [23] coined the word "asphaltene" in France in 1837. Boussingault described the constituents of some bitumens found at that time in eastern France and in Peru. He named it the fraction of distillation residue, which was insoluble in alcohol and soluble in essence of turpentine, "asphaltene," since it resembled the original asphalt. The strong interest in developing a better understanding of the solution behavior of asphaltenes has been motivated by their impact on production, transportation, refinement and utilization of petroleum. The asphaltene fraction is composed of the heaviest components in crude oils. Separated solid asphaltenes usually appear brown to black and have no definite melting point but decompose when the temperature exceeds 300-400 °C. It has been shown that changes in temperature [24,25], pressure [26-28] and oil composition [29] can cause asphaltene precipitation. Asphaltenes are flat sheets of condensed polyaromatic hydrocarbons interconnected with sulfide, ether, aliphatic chain, and naphthenic ring linkages [30,31]. The edges of the sheet consist of alkyl chains.

Resins are defined as the non-volatile and the polar fraction of crude oil that is soluble in n-alkenes (i.e., pentane) and aromatic solvents (i.e., toluene) and insoluble in liquid propane. They are structurally similar to asphaltenes; on the other hand, molar mass is lower, hydrogen/carbon ratio higher, and the heteroatom content lower. Resins are structurally similar to typical surface-active molecules. One end is hydrophilic, with the polar functional groups; the other is hydrophobic, consisting of alkyl chains. In the nonpolar oil environment, the polar end of the resins interacts with exposed cores of asphaltenes, leaving the nonpolar end of the resins to interact with the crude oil medium.

Many excellent studies have discussed the role the asphaltene and asphaltene-resin interactions play in the stabilization of water-in-oil emulsions [7,20,22,32-36].

THEORY

1. Stage Process/Mechanism

The coalescence between drops in an immiscible liquid medium, or between a drop and its own bulk phase occurs in three stages [12,37-39]. In the first stage, the drops approach each other and are separated by a film of the continuous phase. The second stage involves the thinning of this film to reduce the interfacial area. The thinning rate is affected by the capillary pressure and disjoining pressure, and can be retarded due to the Marangoni effect if surfactant is present [40,41]. With high shear rate, the film thinning rate is inversely proportional to the square of drop size [42]. When the film reaches a certain critical thickness, any significant disturbance or instability will cause it to rupture, and coalescence occurs [40,43]. Film thinning is often the overall controlling step. According to Williams and Bailey [44], electrostatic coalescence is a combination of

dipole coalescence and 'migratory coalescence'. Dipole coalescence is due to a dielectrophoretic attractive force between two water drops, from their polarization in the electric field. Migratory coalescence is electrophoresis, relying on the drops being charged. A drop may initially possess electric double-layer charges, as given in:

$$q_d = \frac{4\pi r^2 \varepsilon_1 \varepsilon_0 \zeta}{\delta_{DI}} \tag{1a}$$

Where the double-layer thickness:

$$\delta_{DI} = \left(\frac{K_{dif} \varepsilon_1 \varepsilon_0}{C_m} \right)^{1/2} \tag{1b}$$

Further charging can occur, by contacting an electrode as in [44]:

$$q_i = \left(\frac{\pi^2}{6} \right) 4\pi r^2 \varepsilon_1 \varepsilon_0 E_0 \tag{2}$$

In addition, drops must retain their charges sufficiently long to traverse the distance between the electrodes in the electric field. Electrophoresis, arising from the electrostatic attraction of charged electrodes for charged drops [45], moves the drops in the electric field direction. Migratory coalescence, which usually occurs in a unidirectional field as the direction of droplet motion is fixed, relies on the charge relaxation time τ being long [44]:

$$T = \frac{\varepsilon_1 \varepsilon_0}{C_m} \tag{3}$$

2. Effects of the Applied Electric Field
2-1. Different Kinds of Electric Field
2-1-1. Uniform Electric Field

In this kind of electric field, the two electrodes are placed inside the emulsion. With the passing of an electrical current, a uniform field is composed between the electrodes, and the passage of the current through these two electrodes forms a uniform field and the drops from the dispersed phase move in two of the electrodes.
2-1-2. Non-uniform (Radial) Electric Field

In this kind of electric field, one electrode is put inside the emulsion and the other inside the electrolyte solvent. With the passage of electrical current through the two electrodes, a radial field is composed towards the central electrode. One of the advantages of this kind of field is that the two electrodes do not contact each other, and consequently there is not any short-circuiting because of the composition of water drop chains.
2-2. Dielectrophoresis

Dielectrophoresis (DEP) is the migration of a micro particle in a non-uniform electric field, [46] which is caused by an interaction between an induced dipole in the micro particle and the electric field. "Positive DEP" corresponds to migration in which a micro particle goes to a region of stronger electric field, and "negative DEP" does the opposite phenomenon.

The strength and direction of the DEP force depend on the dielectric properties of both the micro particle and the medium. The time-averaged DEP force ($<F_{DEP}>$) of a spherical particle in an electric field of alternating current (ac) is expressed as [47]:

$$\langle F_{DEP} \rangle = 2\pi r_e^3 \varepsilon_m [K_e] \nabla |E_{rms}|^2 \tag{4}$$

Where $|E_{rms}|^2$ is the squared electric field; the underlining indicates a complex property. Re[ke] is simply written as:

$$\text{Re}[\underline{ke}] \approx \frac{\sigma_p - \sigma_m}{\sigma_p + 2\sigma_m}, \ f < f_{MW}; \ \text{Re}[\underline{ke}] \approx \frac{\varepsilon_p - \varepsilon_m}{\varepsilon_p + 2\varepsilon_m}, \ f > f_{MW} \quad (5)$$

Where subscripts ρ and m are particle and medium, respectively. Positive and negative DEPs correspond to the sign of Re[ke]. The f_{MW} refers to the critical frequency (the so-called Maxwell-Wagner) that differentiates the conductivity regime from the permittivity regime, defined as:

$$f_{MW} = \frac{\sigma_p + 2\sigma_m}{2\pi(\varepsilon_p + 2\varepsilon_m)} \quad (6)$$

3. The Critical Field Strength for Droplet Disintegration

The condition for drop stability is given by Eq. (7) [48]:

$$E_C \leq K_{P1}\left(\frac{\lambda}{r}\right)^{1/2} \quad (7)$$

The critical field strength for droplet disintegration is given by Eq. (8) [18]:

$$E_C = K_{P2}\sqrt{\frac{\lambda}{\varepsilon_1 \varepsilon_0 r}} \quad (8)$$

Above the critical field E_C, the interface becomes unstable and dispersion occurs, producing much finer droplets, with E_C given by Eq. (9) [49]:

$$E_C = 0.64\left(\frac{\lambda}{2\varepsilon_1 \varepsilon_0 r}\right)^{1/2} \quad (9)$$

These equations are all essentially the same but different in their proportionality constants.

According to Miksis [50], the drop shape is determined by its dielectric constant and a dimensionless parameter γ_0 as given by Eq. (10):

$$\gamma_0 = \left(p^{(1)} - \frac{1}{8\pi}\rho\frac{d\varepsilon_1}{d_\rho}(E_1)^2 - P^{(2)}\right)\frac{8\pi}{F^2} \quad (10)$$

For large γ_0, the drop is basically a sphere. As γ_0 decreases from infinity, the drop extends in the direction of the field. At first, it becomes nearly a prolate spheroid. As γ_0 decreases further, it elongates and retains its nearly prolate spheroidal shape if $\varepsilon_1 < \varepsilon_c$, where ε_c is a certain critical value. However, if $\varepsilon_1 > \varepsilon_c$, the drop will develop two obtuse-angled conical points at its ends, known as Taylor cones [51].

EXPERIMENTAL

1. The Method of Preparing the Emulsion

In this way, the used crude oil emulsion was the "Blend Crude Oil" of Kazakhstan having approximate API[‡] types of 39.5 & 32.5 and the water volume fraction of 2 & 6 percent which was measured by the laboratory of Neka[§] Oil Terminal Co. by using ASTM standard.

In the batch apparatus, 300 cc of Xylene should be mixed with 2 cc of fatty oil sulfonated as a demulsifier. Then 5 cc of the result is added to the 300 cc of the sample, and then it should be mixed intensively with the desired temperature over the heater by the magnet to achieve a homogeneous sample. In addition, the oily anticoagulation separation film between the drops should be provoked

by the Xylene and emulsifier and become somewhat weaker. The size of the dispersed drops is about 10-35 μm in this type of oil, measured by the optical microscope.

$$^{\ddagger \circ}\text{API} = \frac{141.5}{\text{Sp.Gr}_{60^\circ F}} - 131.5$$

[§]A town in north of Iran

2. Experimental Set-up and Procedure

The dielectrophoresis separation apparatus consists of three glasses chambers. The central glass chamber includes a sample of emulsion that is visible and controllable from outside and is chosen as the separator chamber. One can assume the apparatus to be a three-cylinder labyrinthine shape, that the central roll or cylinder (the smallest one) contains crude oil, the second cylinder contains 30% sulfuric acid (% by volume), and the external one (the biggest one) is the adjuster of the temperature (water bath).The container includes an emulsion with a diameter of 40 mm, thickness of 1.6 mm, and height of 330 mm that its end is graded with the accuracy of 0.05 cc. This container includes sulfuric acid with the diameter of 70 mm and the height of 320 mm. The tests are applied on a static emulsion and in atmospheric pressure.

To create different voltages, we have used an autotransformer that has the capability of producing AC. In various tests on the sample, this electric current is transmitted to the emulsion sample by two steel electrodes located inside the two separated glass chambers. The first steel electrode is located inside the central cylinder containing crude oil, one end of each attached to a copper wire. Sulfuric acid (H_2SO_4) in the neighboring container is used as a second electrode with a copper wire inside each. Two ends of the copper wire are attached to the autotransformer. The non-uniform (radial) electric field is created after generation of electric current. It is toward the center that is the most powerful field.

By using a small pump inside the water bath in the external chamber, water flows with different temperatures to transfer the heat to the sulfuric acid and crude oil continuously. With the settlement of electric current, the load current is inducted in the external surface of drops. Regardless of the type of the drops' electric charge, they are pulled toward the electrode in which the highest electric field is dominating (metal electrode in center). The flux lines join at the central container that is the representative of the largest electric field in which most of the particle collisions happen. The more distance from the center, the weaker the field intensity.

3. Electrode Specification

In this study, an E7010-A1 steel electrode, with the diameter of 4 mm and the height of 350 mm is used (Table 1).

Electrodes used in this test are of two types: naked and coated-electrode. Coated-electrodes' Teflon thickness is 40 μm.

RESULTS AND DISCUSSION

Temperature condition of 25 °C, 45 °C and 65 °C and electrical

Table 1. Specifications of the applied electrode

C	P	S	Mo	Si	Mn	C
0.1	0.02	0.02	0.5	0.15	0.4	0.1

Table 2. Experimental data for naked electrode/Semi-heavy crude oil

Kind of current	AC current																	
Kind of electrode	Naked electrode																	
Kind of oil	Semi-heavy crude oil (°API=32.5)																	
Water volume fraction	Volume fraction=2%									Volume fraction=6%								
Temperature (°C)	25			45			65			25			45			65		
Voltage (kV)	9	12	15	9	12	15	9	12	15	9	12	15	9	12	15	9	12	15
Separation efficiency (%)	24	34	54	28	43	57	32	54	62	39	56	59	45	63	68	51	73	78

Table 3. Experimental data naked electrode/light crude oil

Kind of current	AC current																	
Kind of electrode	Naked electrode																	
Kind of oil	Light crude oil (°API=39.5)																	
Water volume fraction	Volume fraction=2%									Volume fraction=6%								
Temperature (°C)	25			45			65			25			45			65		
Voltage (kV)	9	12	15	9	12	15	9	12	15	9	12	15	9	12	15	9	12	15
Separation efficiency (%)	29	43	56	33	53	64	42	59	69	44	55	68	53	65	80	55	76	84

Table 4. Experimental data for Teflon-coated electrode/Semi-heavy crude oil

Kind of current	AC current																	
Kind of electrode	Teflon-coated electrode																	
Kind of oil	Semi-heavy crude oil (°API=32.5)																	
Water volume fraction	Volume fraction=2%									Volume fraction=6%								
Temperature (°C)	25			45			65			25			45			65		
Voltage (kV)	9	12	15	9	12	15	9	12	15	9	12	15	9	12	15	9	12	15
Separation efficiency (%)	23	31	47	24	40	54	25	49	62	35	48	59	46	58	77	47	76	81

Table 5. Experimental data for Teflon-coated electrode/light crude oil

Kind of current	AC current																	
Kind of electrode	Teflon-coated electrode																	
Kind of oil	Light crude oil (°API=39.5)																	
Water volume fraction	Volume fraction=2%									Volume fraction=6%								
Temperature (°C)	25			45			65			25			45			65		
Voltage (kV)	9	12	15	9	12	15	9	12	15	9	12	15	9	12	15	9	12	15
Separation efficiency (%)	26	36	56	30	52	61	38	58	66	37	57	76	50	76	85	53	78	87

voltage of 9, 12 and 15 kV were chosen for AC Current. Frequency for all experiments has been 50 Hz and experiment time has been 5 minutes. Separation efficiency is the water volume measured in the central scaled column, divided by the total water volume multiplied by 100.

1. The Effect of Voltage

As shown in Tables 2, 3, 4, 5, the greater the increase separation efficiency occurs in non-uniform electric field for the AC current, the more voltage is increasing. In this method, the largest electric field is in the center, where the metallic electrode is. This is due to the voltage gradient and greater accumulation of electric flux in the center, which have a great effect on the separation efficiency. Although quantitatively depending on the type of electrode covering, the type of oil, the value of volume fraction and temperature, the separation efficiency always increases upon increasing voltage. Nevertheless, it is noticeable that in very high intensity of field the reverse effect happens, which results in drop breakage. The effect of electric field is not usually constant, due to different ion species and the used solvent and it depends on the physical and superficial properties of the system.

2. The Effect of Water-phase Volume Fraction

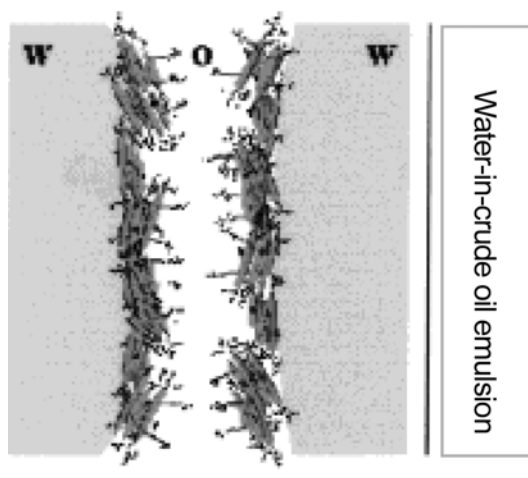The effect of volume fraction on the separation efficiency for elec-

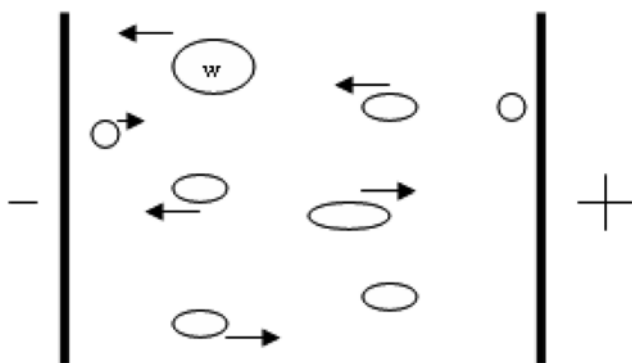**Fig. 1. In the absence of particles, resin/asphaltene films stabilize water-in-oil emulsions.**

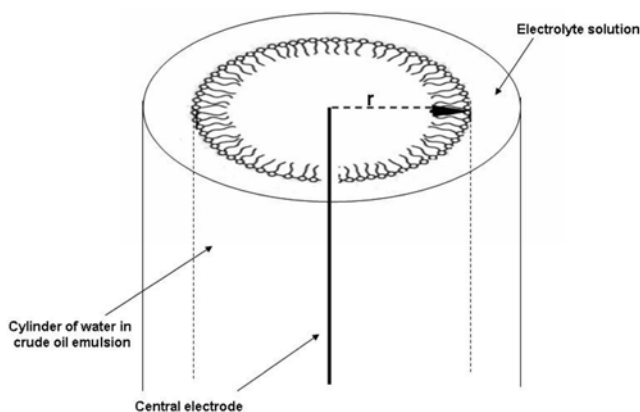**Fig. 2. The schematic diagram of a uniform electric field.**

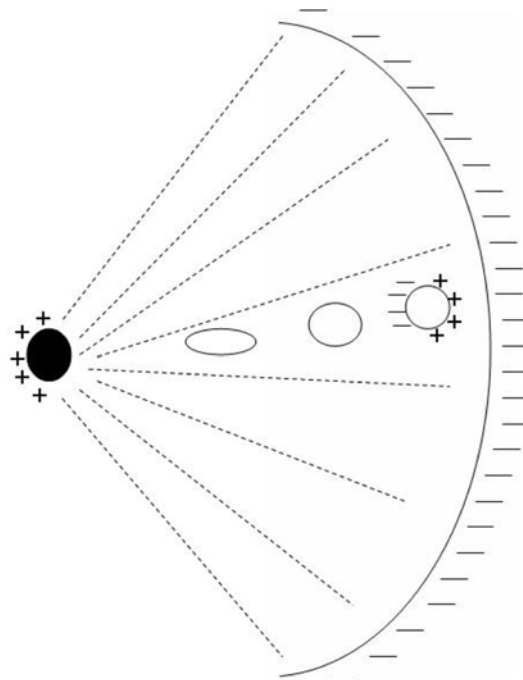**Fig. 3. The schematic diagram of a non-uniform electric field.**

Fig. 4. The schematic diagram of positive dielectrophoresis flux.

Fig. 5. The schematic diagram of the electrical separation apparatus.

trical voltage of 15 kV and different temperatures in a non-uniform field is shown in Fig. 6. Considering the figure, it is clear that the yield of separation increases when water volume fraction increases. This is due to the increase in number and size of drops. It will also affect the polarization charge that can be induced on each drop for a given electric field and frequency. Hence, the volume fraction has an effect on the collision rate of the drops and the coalescence pa-

rameter. Although quantitatively depending on the type of oil, temperature and electrode covering, the separation efficiency is always an increasing volume fraction.
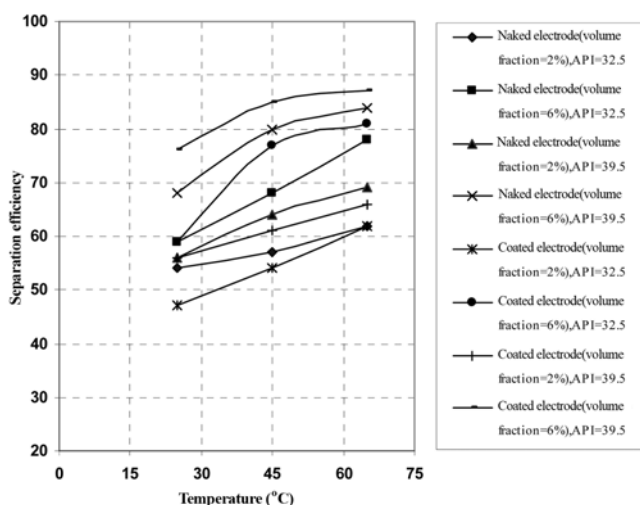
Fig. 6. The effect of water volume fraction changes (dispersed phase) on separation efficiency.
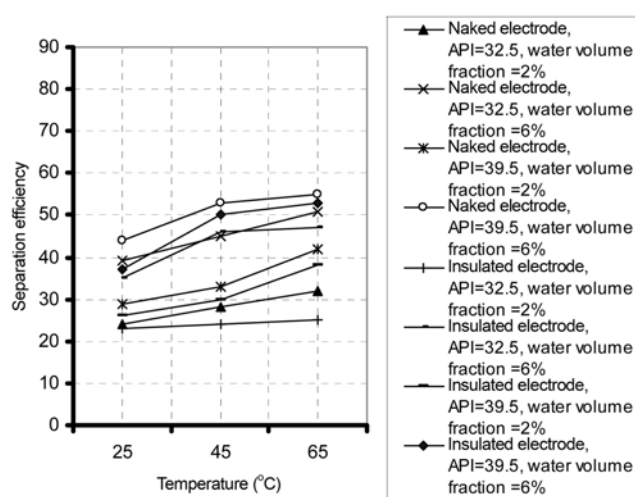

Fig. 8. The effect of temperature changes on separation efficiency (voltage=9 kV).
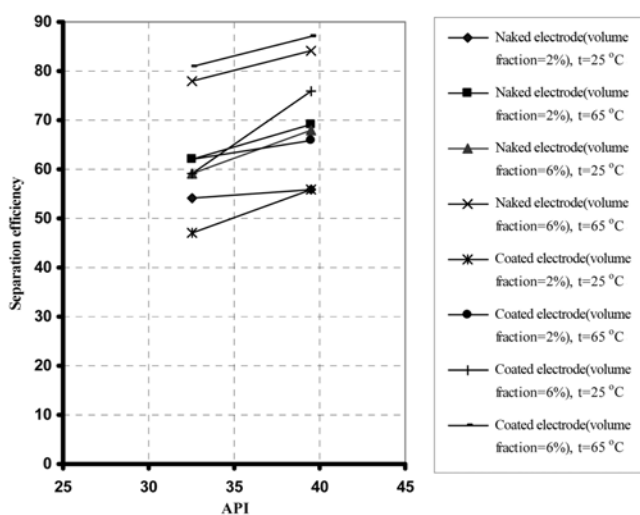

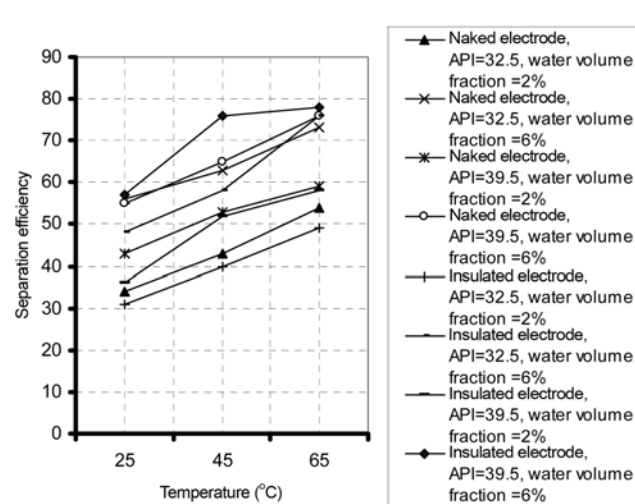Fig. 7. The effect of API changes on separation efficiency for AC current.

Fig. 9. The effect of temperature changes on separation efficiency (voltage=12 kV).

3. The Effect of API

Effect of API on the separation efficiency for electrical voltage of 15 kV, temperature of 65 °C and 25 °C, water volume fraction of 2% and 6% and in a non-uniform electric field is shown in Fig. 7. Considering the figure mentioned, it is obvious that the rate of separation increases by increasing API or decreasing specific gravity of crude oil. It happens because the water particles' motion to the center of the electric field becomes more facilitated due to the lower oil density. Thus, as mentioned previously in the first section, the amount of asphaltene in light oils is less than in heavy ones, so the oily surrounding film breaks easier and causes more collision and the separation efficiency subsequently increases.

4. The Effect of Temperature

The effect of temperature changes on separation efficiency for different voltages in a non-uniform electric field with the AC current is shown in Figs. 8 to 10. With corresponding figures, it is obvious that the separation process will be more efficient when the temperature gets higher up to 65 °C. This happens because the more
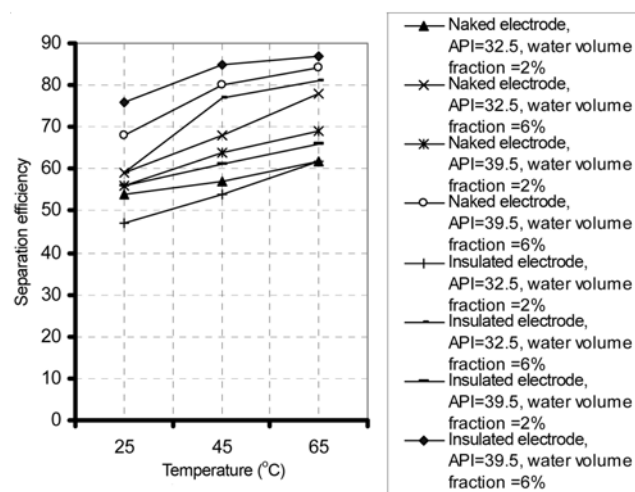

Fig. 10. The effect of temperature changes on separation efficiency (voltage=15 kV).

particle motion increases, the more temperature increases; thus the number of collisions in a specific time increases and the separation efficiency and settling subsequently increases. Likewise, surrounding film around the drop, which is a composition of asphaltene, resin, paraffin, etc., will be excited and its complicated structure becomes weak and will break with the first electric shock and at the beginning of drop deformation. The experiment's time for all temperatures is five minutes. Although quantitatively depending on the kind of electrode covering, type of oil, volume fraction, the separation efficiency always increases upon increasing temperature.

It is very important to note that two kinds of problem can emerge due to heating. One is the light components, which determines the price of crude oil, vaporize on heating and decrease the treated crude oil price. The other disadvantage is the decline of the separation efficiency due to the formed air bubbles. The air bubbles formed by heating can absorb surface-active components [52] and also adhere to the surface of water drops and decrease the apparent viscosity of the drops. These drops are not removed by sedimentation; they act as oil with low density and come out from the electrostatic dehydrator without being removed. Thus, it is important to choose the appropriate temperature in the demulsification process to prevent these problems [53].

DETERMINATION OF EXPERIMENTAL MODEL BY EXPERIMENTAL DATA

The correlating equation of the demulsification kinetics was derived as follows by summarizing the experimental results obtained in the preceding section. The mathematical calculations were performed by a combination of regression & Mont Carlo techniques:

For AC voltage both naked and Teflon coated electrodes:

$$\frac{Y}{100} = AX + BX^2 + CX^3, \quad X = \left(\frac{H}{2}\right)^{\alpha}\left(\frac{T}{25}\right)^{\beta}\left(\frac{V}{12}\right)^{Y}$$

For Teflon coated electrode:

$$\begin{cases} \alpha = 0.3589 \\ \beta = 0.3716 \\ Y = 1.3578 \end{cases}, \begin{cases} A = -0.052253 + 0.009814 \times (^{\circ}API) \\ B = -0.062335 + 0.004143 \times (^{\circ}API) \\ C = 0.000640703 - 0.00095714 \times (^{\circ}API) \end{cases}$$

Mare=5.1%

$$\text{Mare} = \frac{\sum_{i=1}^{n}\left|\frac{Y_{cali} - Y_{expi}}{Y_{expi}}\right|}{N} = \text{Mean absolute relative error}$$

For naked electrode:

$$\begin{cases} \alpha = 0.5327 \\ \beta = 0.4474 \\ Y = 1.9121 \end{cases}, \begin{cases} A = 0.034586 + 0.01371 \times (^{\circ}API) \\ B = 0.101345 - 0.00067429 \times (^{\circ}API) \\ C = -0.0314 + 0.0001 \times (^{\circ}API) \end{cases}$$

Mare=4.0%

CONCLUSION

The demulsification process in crude oil recovery has been simulated with the field strength, volume fraction, demulsifier, temperature, API and type of electrode (coated or naked). A model emulsion of water-in-crude oil type containing 6% of water from Kazakhstan

as "Blend crude oil" was prepared, with the size of the water droplets being about 10-35 µm.

Using a batch electrostatic dehydrator, the demulsification rates of water-in-crude oil emulsion in radial electric field and in high AC current were investigated under various conditions.

1. The water separation efficiency increases with the non-uniform electric field because of increasing electrostatic force among droplets. This is due to the voltage gradient and greater accumulation of electric flux in the center, which have a great effect on the separation efficiency.

2. By using non-uniform electric field and coated electrode, short-circuiting between electrodes is impossible.

3. The water separation efficiency increase by temperature may be attributed mainly to the decrease in crude oil viscosity and excitement of oil film around the drop that breaks with the first electric shock and during the beginning of drop deformation.

4. The water separation efficiency increase by °API (decreasing Sp.Gr) may be attributed to the amount of asphaltene, which in light oils is less than in heavy oils. So the oily surrounding film breaks easier and causes more collisions and the separation efficiency increases subsequently.

5. By increasing the water volume fraction, the rate of separation (in light oil) increases with the value of 21% for the coated electrode and 15% for the naked electrode. This is due to the increase in number and size of drops. It will also affect the polarization charge that can be induced on each drop in an electric field.

ACKNOWLEDGMENT

NOMENCLATURE

C_m : medium conductivity [S/m]
E_c : critical electric field at the drop surface [V/m]
E_0 : applied electric field [V/m]
E_1 : the field inside the drop [V/m]
E_{rms} : electric field intensity (rms: root mean square) [V/m]
f : frequency of ac [s⁻¹]
f_{MW} : critical frequency [s⁻¹]
F : the force attracting the two surfaces together [N]
K_{dif} : coefficient of diffusion [m²/s]
K_{P1} : proportionality constant
K_{P2} : proportionality constant
$P^{(1)}$: pressure inside a drop [Pa]
$P^{(2)}$: pressure outside a drop [Pa]
q_d : double-layer charge of a drop [C]
q_i : charge of a drop due to contact charging [C]
r : droplet radius [m]
$R_e[\underline{K_e}]$: real part of the Clausius-Mossotti factor [Ke]
A : coefficient
B : coefficient
C : coefficient
Y : separation efficiency
V : voltage [kV]

H   : volume fraction [% by volume]
T   : temperature [ºC]
N   : number of experimental data

Greek Letters
γ_0 : dimensionless parameter
δ_{DL} : double-layer thickness [m]
ε_0 : permittivity of vacuum [F/m]
ε_1 : dielectric constant of continuous phase
ε_m : permittivity of the medium
ζ : zeta-potential of particles [V]
ρ : mass density [kg/m^3]
σ : conductivity
τ : charge relaxation time [s]
∇ : del vector
γ : constant parameter
α : constant parameter
β : constant parameter

REFERENCES

1. C. M. Blair, *Chem. Ind.*, 538 (1960).
2. R. A. Mohammed, A. I. Bailey, P. F. Luckham and S E. Taylor, *Colloids Surf. A: Physicochem. Eng. Aspects*, **80**, 223 (1993).
3. T. J. Jones, E. L. Neustadter and K. P. Whittingham, *J. Can. Pet. Technol.*, **17**, 100 (1978).
4. D. T. Wasan, *Destabilization of water-in-oil emulsions*, In *Emulsion's A* Fundamental and Practical Approach; Sjoblom, J., Ed., Kluwer Academic Publishers: Dordrecht, The Netherlands, 283 (1992).
5. R. J. R. Cairns, D. M. Grist and E. L. Neustadter, *Theory and practice of emulsion technology*, Smith, A. L., Ed., Academic Press, New York, 135 (1974).
6. O. K. Kimbler, R. L. Reed and I. H. Silberberg, *SPE J.*, 153 (1966).
7. S. E. Taylor, *Chem. Ind.*, **20**, 770 (1992).
8. O. Urdahl and J. Sjöblom, *J. Dispersion Sci. Technol.*, **16**, 557 (1995).
9. R. A. Mohammed, A. I. Bailey, P. F. Luckham and S. E. Taylor, *Colloids Surf. A: Physicochem. Eng. Aspects*, **91**, 129 (1994).
10. C. S. Shetty, A. D. Nikolov and D. T. Wasan, *J. Dispersion Sci. Technol.*, **13**, 121 (1992).
11. K. J. Lissant, *Demulsification: Industriel application, Surfactant Science Series*, Vol. 13, Marcel Dekker, New York (1983).
12. D. Sun, S. C. Jong, X. D. Duan and D. Zhou, *Colloids Surf. A*, **150**, 69 (1999).
13. M. Goto, J. Irie, K. Kondo and F. Nakashio, *J. Chem. Eng. Japan*, **22**(4), 401 (1989).
14. H., N. Ino, M. Imaishi, Hozawa and K. Fujinawa, *Kagaku Kogaku Ronbunshu*, **9**, 263 (1983).
15. A. Kriechbaumer and R. Marr, Macro- and Micro-emulsion (ACS Symp. Ser, 272, Ed. By D.O. Shah). Am. Chem. Soc., U.S.A, 381 (1985).
16. M. Yamaguchi, A. Kobayashi and T. Katayama, *Kagaku Kogaku Ronbunshu*, **11**, 729 (1985).
17. K. Yoshizuka, K. Kondo and F. Nakashio, *J. Chem. Eng. Japan*, **19**, 396 (1986).
18. S. E. Taylor, *Trans. IChemE*, **74**(A), 526 (1996).
19. D. D. Eley, M. J. Hey and M. A. Lee, *Colloids Surf.*, **24**, 173 (1987).
20. E. J. Johansen, I. M. Skjarvo, T. Lund, J. Sjoblom, H. Soderlund and

G. Bostrom, *Colloids Surf.*, **34**, 353 (1989).
21. Y. H. Kim, D. T. Wasan and P. J. Breen, *Colloids Surf. A: Physicochem. Eng. Aspects*, **95**, 235 (1995).
22. I. R. Mansurov, E. Z. Il'yasova and V. P. Vygovskoi, *Chem. Technol. Fuels Oils*, **23**, 96 (1987).
23. J. B. Boussingault, *Ann. Chem. Phys.*, **64**, 141 (1837).
24. L. H. Ali and K. A. Al-Ghannam, *Fuel*, **60**, 1043 (1981).
25. B. J. Fuhr, C. Cathrea, L. Coates, H. Kalra and A. I. Majeed, *Fuel*, **70**, 1293 (1991).
26. N. B. Joshi, O. C. Mullins, J. Abdul, J. Creek and J. McFadden, *Energy & Fuels*, **15**, 979 (2001).
27. A. Hirschberg, L. N. J. DeJong, B. A. Schipper and J. G. Meijer, *Soc. Pet. Eng. J.*, **24**(3), 283 (1984).
28. H. Laux, I. Rahimian and D. Browarzik, *Petroleum Science and Technology*, **19**(9&10), 1155 (2001).
29. E. Y. Sheu, *J. Phys. Condens. Matter*, **8**(25A), A125 (1996).
30. R. Pelet, F. Behar and J. Monin, *Org. Geochem.*, **10**, 481 (1985).
31. T. F. Yen, *Fuel Sci. Technol. Int.*, **10**, 723 (1992).
32. H. Fordedal, Ø. Midttun, J. Sjöblom, O. K. Kvalheim, Y. Schildberg and J.-L. Volle, *J. Colloid Interf. Sci.*, **182**, 117 (1996).
33. G. D. M. Mackay, A. Y. McLean, O. J. Betancourt and B. D. Johnson, *J. Inst. Pet.*, **59**, 164 (1973).
34. J. Sjoblom, O. Urdahl, H. Hoiland, A. A. Christy and E. J. Johansen, *Prog. Colloid Polym. Sci.*, **82**, 131 (1990).
35. J. Sjoblom, O. Urdahl, K. G. N. Borve, L. Mingyuan, J. O. Saeten, A. A. Christy and T. Gu, *Adv. Colloid Interf. Sci.*, **41**, 241 (1992).
36. E. Y. Sheu, D. A. Storm and M. B. Shields, *Fuel*, **74**, 1475 (1995).
37. C. T. Chen, J. R. Maa, Y. M. Yang and C. H. Chang, *Surf. Sci.*, **406**, 167 (1998).
38. C. C. Man, A. W. Pacek and A. W. Nienow, *IChemE Jubilee Res. Event*, 356 (1997).
39. D. Sun, X. Duan, W. Li and D. Zhou, *J. Membrane Sci.*, **146**, 65 (1998).
40. E. E. Isaacs and R. S. Chow, *Adv. Chem. Ser.*, **231**, 251 (1992).
41. W. Rommel, W. Meon and E. Blass, *Sep. Sci. Technol.*, **27**(2), 129 (1992).
42. A. Bhardwaj and S. Hartland, *J. Disp. Sci. Technol.*, **15**(2), 133 (1994).
43. S. E. Friberg and S. Jones, *Emulsions, in: Kirk-Othmer encyclopedia of chemical technology*, Inc. Vol. 9, 4th Ed., John Wiley & Sons, 393 (1996).
44. T. J. Williams and A. G. Bailey, *IEEE Trans. Ind. Appl.*, **1A-22**(3), 536 (1986).
45. H. A. Pohl, *J. Appl. Phys.*, **22**(7), 869 (1951).
46. H. A. Pohl, *Dielectrophoresis*, Cambridge University Press, Cambridge, 1978 (1983).
47. L. Benguigui and I. J. Lin, *J. Appl. Phys.*, **53**, 1141 (1983).
48. L. C. Waterman, *Chem. Eng. Prog.*, **61**(10), 51 (1965).
49. P. Atten, *J. Electrostatics*, **30**, 259 (1993).
50. M. J. Miksis, *Phys. Fluids*, **24**(11), 1967 (1981).
51. G. Taylor, *Proc. R. Soc. A*, **280**, 383 (1964).
52. J.-Y. Kim, M.-G. Song and J.-D. Kim, *J. Colloid Interf. Sci.*, **223**(2), 285 (2000).
53. B.-Y. Kim, J.-H. Moon and T.-H, Sung, *Separation Sci. & Tech.*, **37**(6), 1307 (2002).
54. R. A. Mohammed, A. I. Bailey, P. F. Luckham and S. E. Taylor, *Colloids Surf. A*, **83**, 261 (1994).